Original Article
J. Korean Wood Sci. Technol. 2025, 53(6): 563-584
https://doi.org/10.5658/WOOD.2025.53.6.563

Journal of the Korean Wood Science and Technology
pISSN: 1017-0715 eISSN: 2233-7180
http://www.woodj.org

Experimental Investigation on the Neutral Axis of Wulung Bamboo (*Gigantochloa Atroviolacea*) BEAM

Inggar Septhia IRAWATI[1,†] · Habib Zainal ARIFIN[1] · Ditya RAMADHANTI[1] · Gatra Dewa OKTANANDA[1] · Shafira Khairunnisa SUBCHAN[1]

ABSTRACT

Previous studies have demonstrated that bamboo exhibits distinct mechanical properties under tensile and compressive loading, characterized by differing moduli of elasticity. This asymmetry implies that the neutral axis of a bamboo cross-section under bending should not lie at mid-height. However, experimental validation of the neutral axis position remains limited. This study aims to comprehensively investigate the bending behavior of Wulung bamboo by considering the tensile and compressive elastic moduli parallel to the grain. Tensile, compressive, and flexural tests were performed according to ISO 22157:2019. The results revealed that the average tensile modulus of elasticity was 15,789 MPa for internodes and 13,716 MPa for nodes, while the average compressive modulus of elasticity was 21,270 MPa and 15,264 MPa, respectively. The neutral axis was consistently located below the geometric center of the cross-section, ranging from approximately –0.03D to –0.09D, where D is the average outer diameter of the bamboo culm. A modification factor for the tensile and compressive elasticity moduli was introduced to achieve internal force equilibrium in flexural analysis. A finite element analysis is recommended to further simulate the interaction between the position of the neutral axis, the modified tensile and compressive elastic moduli parallel to the grain, and the overall flexural behavior of the bamboo. ISO 22156:2021 remains applicable at the design stage, provided material behavior remains within the linear-elastic domain. However, a more detailed analysis of the stress-strain distribution along the fiber direction would help support and refine the structural design process.

Keywords: bending behavior, bending properties, strain distribution, tensile properties parallel to grain, compressive properties parallel to grain

1. INTRODUCTION

Bamboo is a highly versatile and sustainable material that has been utilized for centuries in various human activities. It is particularly valued for its rapid growth and short maturation cycle of 3−5 years (Eratodi, 2017). In recent years, modern bamboo construction has garnered increasing global interest, with notable examples including the Sharma Springs openwork bamboo house in Bali, Indonesia; the bamboo pedestrian bridge in Matina Municipality, Davao, Philippines; the Crosswaters Ecolodge bamboo bridge in China; and bamboo mattresses used to enhance soil bearing capacity in Jombang and Madiun, East Java, Indonesia (Fitrianto, 2015; Lapina and Zakieva, 2021; Medina Yor Maikol *et al.*, 2020; Ready *et al.*, 2020). Bamboo can serve both non-struc-

Date Received April 25, 2025; Date Revised June 6, 2025; Date Accepted July 1, 2025; Published November 25, 2025
[1] Department of Civil and Environmental Engineering, Universitas Gadjah Mada, Yogyakarta 55281, Indonesia
[†] Corresponding author: Inggar Septhia IRAWATI (e-mail: inggar_septhia@ugm.ac.id, https://orcid.org/0009-0003-1222-4327)

tural and structural functions, highlighting the importance of understanding its physical and mechanical characteristics in structural applications. Numerous experimental studies have investigated its tensile, compressive, and flexural performance, as summarized in Tables 1–3.

Tables 1 and 2 show that bamboo exhibits different mechanical properties in tension and compression parallel to the grain. Theoretically, these differences cause the neutral axis in bamboo culm beams to shift away from the centroidal axis (Tian *et al.*, 2021). However, a review of Tables 1–3 reveals a lack of comprehensive experimental studies that investigate the interrelation of tensile and compressive strengths parallel to the grain with flexural behavior, particularly concerning the determination of the neutral axis position and prediction of the normal stress distribution across the cross-section. Gauss *et al.* (2019) observed the neutral axis of bamboo split under flexural loads, but not specifically in culm-shaped bamboo beams. Additionally, Li *et al.* (2024) observed strain distribution across the entire section of I-shaped laminated bamboo, enabling identification of the neutral axis location.

Bamboo is considered a linear and homogeneous material in the design of bamboo beam structures. In

Table 1. Previous research on tensile properties

Previous research	Bamboo species	Tensile properties	
		Strength (MPa)	Modulus of elasticity (MPa)
Gunawan *et al.* (2015)	*Dendrocalamus asper* with node (top part)	197.28*	4,320
	D. asper with node (middle part)	243.81*	3,128
	D. asper with node (bottom part)	169.03*	1,810
	D. asper without node (top part)	313.93*	5,916
	D. asper without node (middle part)	260.37*	5,505
	D. asper without node (bottom part)	250.21*	2,139.67
Widoyoko (2018)	Wulung bamboo without node	250.14*	23,240
Gauss *et al.* (2019)	Brazilian *Phyllostachys edulis* bamboo with a node	100*	11,190
	Brazilian *P. edulis* bamboo without nodes	275*	17,740
Lubis (2019)	Wulung bamboo with a node	92.40*	13,222
	Wulung bamboo without nodes	195.30*	18,576
De Jesus *et al.* (2021)	*D. asper*	242.75–470.06	-
	D. asper	168.80–356.93	-
Cai *et al.* (2023)	Moso bamboo with a node	103.91–120.34	8,472–9,101
	Moso bamboo without nodes	177.80–189.76	7,475–8,216
Meng *et al.* (2023)	Moso bamboo with a node	73.66–85.74	-
	Moso bamboo without nodes	134.83–76.66	-
Li *et al.* (2024)	Laminated Moso bamboo	77.18*	7,777

* Average.

Table 2. Previous research on compressive properties

Previous research	Bamboo species	Compressive properties	
		Strength	Modulus of elasticity
		(MPa)	(MPa)
Hoque *et al.* (2019)	Bangladeshi green bamboo with a node	26.3–54.18	2,300–8,500
	Bangladeshi green bamboo without nodes	18.93–23	300–1,100
Gauss *et al.* (2019)	Brazilian *Phyllostachys edulis* bamboo with a node	59.5*	20,640*
	Brazilian *P. edulis* bamboo without nodes	57.5*	20,380*
Lubis (2019)	Wulung bamboo with a node	53.44*	15,482*
	Wulung bamboo without nodes	56.37*	13,891*
De Jesus *et al.* (2021)	*D. asper* with node	44.83–63.21	-
	D. asper without node node	43.83–69.60	-
Liu *et al.* (2021)	Moso bamboo with a node	59.80*	-
	Moso bamboo without nodes	57.20*	-
Hartono *et al.* (2022)	*D. asper*	41–50	-
Meng *et al.* (2023)	Moso bamboo with a node	32.03–48	-
	Moso bamboo without nodes	30.07–47.71	-
Li *et al.* (2024)	Laminated Moso bamboo	59.74*	9,777*

* Average.

addition, the tensile modulus of elasticity is assumed to be the same as the compressive modulus of elasticity (International Organization for Standardization, 2021b). Therefore, in the calculation of bamboo beam design, the neutral axis is located at 1/2 the diameter of the bamboo. For design purposes, this assumption may be sufficient. However, along with the development of science, a study of the behavior of bamboo beams that considers mechanical properties closer to reality is needed. Therefore, this study aims to experimentally investigate the position of the neutral line in bamboo beams. The bamboo used in this study is Wulung bamboo (*Gigantochloa atroviolacea*), which is commonly used for building structures in Indonesia (Irnawan, 2022).

Tensile, compression, and bending tests were performed according to ISO 22157:2019. The results of the will provide comprehensive information about the load–deflection curve, strain distribution in the cross-section of the bamboo beam at mid-span, neutral axis position in the cross-section of the bamboo beam at mid-span, modulus of rupture, tensile strength, compressive strength, and flexural, tensile, and compressive elastic moduli. These findings will be valuable input for future numerical analysis and contribute to the development of more accurate computational models for simulating the flexural behaviour of bamboo structures.

2. MATERIALS and METHODS

The bamboo species utilized in this study was Wulung bamboo (*G. atroviolacea*), which was sourced from Yogyakarta, Indonesia. The selected bamboo

Table 3. Previous research on bending behaviour

Previous research	Brief description
Kim *et al.* (2018)	A study was conducted to evaluate the effect of span length on the bending properties of larch lumber. Two types of specimens were used, with lengths of 1,650 mm and 3,000 mm. The observed parameters included bending strength and modulus of elasticity.
Lee *et al.* (2018)	The longitudinal bond strength of larch wood was assessed through experimental testing. Six types of end-joint specimens were examined, with each joint located at the mid-span of the beam. Observations included failure modes, load–deflection responses, and calculations of flexural strength and modulus of elasticity.
Maulana *et al.* (2019)	Static and dynamic bending tests were performed on oriented strand boards (OSBs) made from *Dendrocalamus asper* under various shelling ratios. The evaluated properties included static bending strength, static modulus of elasticity (MOE), and dynamic modulus of elasticity. The correlation between static and dynamic MOE was also examined.
Galih *et al.* (2020)	Bending tests were conducted to evaluate the mechanical performance of tropical hybrid cross-laminated timber (CLT). The core layer consisted of bamboo laminated board made from *P. edulis*, while the face layers were composed of rubberwood (*Hevea brasiliensis*) and jelutong (*Dyera costulata*). The primary properties investigated were bending strength and modulus of elasticity.
Iswanto *et al.* (2020)	Sandwich particleboards were investigated for their potential application as building acoustic materials. The boards were fabricated using *Gigantochloa pruriens* and *Gigantochloa apus*. In this study, the bending strength and modulus of elasticity were evaluated.
Deng and Peng (2021)	An experimental study was conducted to investigate the bending properties of Moso bamboo (*P. edulis*). The data collected included load–deflection and load–strain curves, bending strength, and elastic modulus. However, the position of the neutral axis was not addressed in the study.
Wang *et al.* (2023)	Experimental and numerical studies were carried out to investigate the effect of nodes on the flexural behavior of Moso bamboo (*P. edulis*). The comparison focused on the load–deflection curves obtained from both the experimental tests and finite element analysis. In the experimental study, strain measurements were not conducted; only the load–deflection response was recorded.
Zhang *et al.* (2024)	The effect of load duration on the flexural strength of InorgBam was evaluated under long-term loading conditions. The specimens were fabricated using Moso bamboo (*P. edulis*) and bonded with magnesium oxysulfide adhesive. The experimental results captured the relationship between flexural strength and load duration.
Li *et al.* (2024)	An experimental study was conducted on I-shaped laminated bamboo members. The investigation included observations of failure modes, strain distribution, load–deflection behavior, elastic proportional limit, ultimate limit, and failure limit. However, tensile and compressive tests parallel to the grain were not performed, which prevented a detailed analysis of stress distribution.
Rofii *et al.* (2024)	The bending properties of laminated boards made from Petung bamboo (*D. asper*) were investigated. Flexural tests were conducted to determine the bending strength and modulus of elasticity.
Sumardi *et al.* (2022)	Experimental studies were conducted on bamboo zephyr composites made from *G. apus* and falcata veneer. The objective of the study was to determine the bending strength and modulus of elasticity.
Awaludin *et al.* (2025)	The flexural properties of glulam beams made from various wood species—including Jabon, Pine, Mahogany, Mangium, Rubberwood, Merbau, Keruing, Meranti Batu, and Bangkirai—were investigated. The experimental results included load–deflection curves, bending strength, and modulus of elasticity.

culms, aged between 3 to 5 years, were designated as Bamboo 1, Bamboo 2, and Bamboo 3. Their geometric properties are presented in Table 4. The lengths of Bamboo 1, Bamboo 2, and Bamboo 3 are 6,245 mm, 6,240 mm, and 6,385 mm, respectively, with each culm comprising 16, 17, and 16 nodes. As shown in Table 4,

Table 4. Initial measurement of bamboo dimensions

Speciment	Length (mm)	Diameter (mm)				Number of nodes
		Bottom	Middle	Top	Average	
Bamboo 1	624.5	89	82.5	79.6	83.7	16
Bamboo 2	624	89.6	84.4	78.6	84.2	17
Bamboo 3	638.5	89	80	70	79.7	16

the bamboo culms exhibit a non-prismatic geometry, characterized by a larger diameter at the base compared to the top.

The bamboo culms were preserved using vertical soak diffusion in a 0.2% deltamethrin solution, followed by air-drying for six months to achieve equilibrium moisture content. The relative humidity and temperature of the bamboo storage room were 85.33% and 26.05℃, respectively. After conditioning, specimens for tensile, compressive, and bending tests were prepared by cutting the culms at predetermined positions in accordance with the dimensional specifications outlined in ISO 22157: 2019. The cutting positions are illustrated in Fig. 1. The resulting tensile, compressive, and bending specimens are summarized in Table 5. Due to the limited length of the bamboo culms, the number of tensile specimens obtained from Bamboo 1, Bamboo 2, and Bamboo 3 was four, two, and two, respectively. The number of compressive specimens from Bamboo 1, 2, and 3 was two, one, and two, respectively. For the bending test, one specimen was prepared from each bamboo culm.

Tensile specimens were prepared in accordance with ISO 22157:2019. Their geometric configuration is illustrated in Fig. 2, and additional dimensional data are provided in Table 6. The specimen thicknesses ranged from 1.8 mm to 3.4 mm, with a gauge length of 50 mm for the tensile section. Hardwood tabs were affixed to both ends of each specimen to ensure proper gripping during testing. The tensile tests were performed using a universal testing machine, with the loading rate adjusted to produce failure within 300 ± 120 seconds.

The compressive test specimens were also prepared in accordance with ISO 22157:2019. The specimen dimensions are illustrated in Fig. 3 and further detailed in Table 7. The height of each compressive specimen was approximately equal to the outer diameter of the bamboo cross-section. Compressive testing was carried out using a universal compression testing machine, with a loading rate to induce failure within 300 ± 120 seconds, similar to the tensile test procedure.

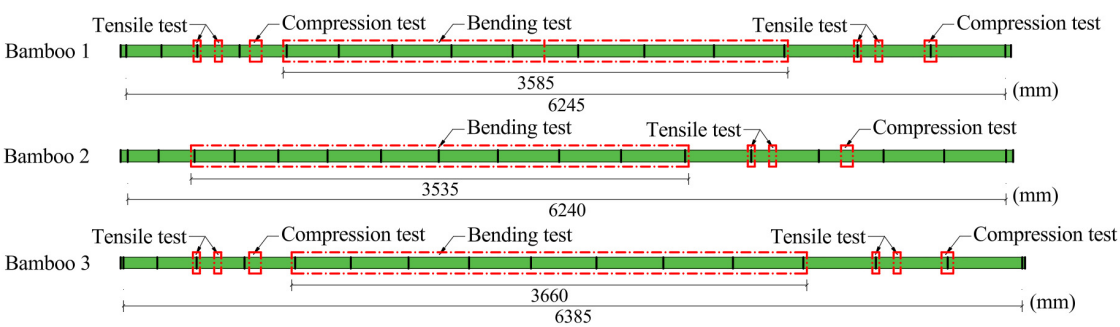

Fig. 1. Cutting positions of bamboo culms.

Table 5. Test specimen of bending, tensile, and compressive tests

Test	Position	Notation		
		Bamboo 1	Bamboo 2	Bamboo 3
Tensile test with node	Bottom-part	$B_{t\text{-}bn}1$	-	$B_{t\text{-}bn}3$
Tensile test with node	Top-part	$B_{t\text{-}tn}1$	$B_{t\text{-}tn}2$	$B_{t\text{-}tn}3$
Tensile test without node	Bottom-part	$B_{t\text{-}bi}1$		$B_{t\text{-}bi}3$
Tensile test without node	Top-part	$B_{t\text{-}ti}1$	$B_{t\text{-}ti}2$	$B_{t\text{-}ti}3$
Compression test without node	Bottom-part	$B_{c\text{-}bi}1$	-	$B_{c\text{-}bi}3$
Compression test without node	Top-part	-	$B_{c\text{-}ti}2$	-
Compression test with node	Bottom-part	-	-	-
Compression test with node	Top-part	$B_{c\text{-}tn}1$	-	$B_{c\text{-}tn}3$
Bending test	Middle part	B_b1	B_b2	B_b3

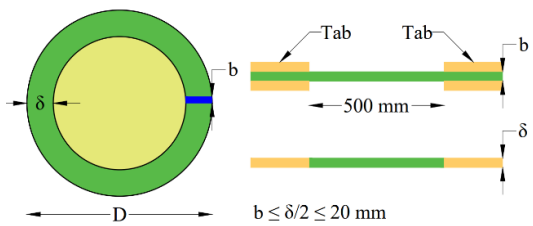

Fig. 2. Tensile test specimen dimension according to ISO 22157:2019.

Bending test specimens were prepared from the same bamboo culms used for tensile and compressive testing. The specimen dimensions are presented in Table 8. The bending testing setups B_b1, B_b2, and B_b3 are illustrated in Figs. 4–6, respectively. These Figures show the load application points, support saddle, loading saddle, and the positions of linear variable differential transformer (LVDT). Four strain gauges were installed at the mid-span of each bamboo beam, with their positions on the

Table 6. Measurement of tensile test specimens

Speciment	Code	Width [b (mm)]		Thickness [t (mm)]		Length (mm)
		b_1	b_2	t_1	t_2	L
Bamboo 1	$B_{t\text{-}bi}1$	12.00	11.50	3.40	3.30	50.00
	$B_{t\text{-}bn}1$	14.40	12.80	2.70	3.35	50.00
	$B_{t\text{-}ti}1$	8.25	8.00	2.70	2.70	50.00
	$B_{t\text{-}tn}1$	11.00	9.60	2.95	2.95	50.00
Bamboo 2	$B_{t\text{-}ti}2$	9.05	9.10	1.90	2.10	50.00
	$B_{t\text{-}tn}2$	10.00	10.30	2.50	2.50	50.00
Bamboo 3	$B_{t\text{-}bi}3$	11.90	11.55	2.45	2.45	50.00
	$B_{t\text{-}bn}3$	13.35	13.35	2.60	2.10	50.00
	$B_{t\text{-}ti}3$	7.15	7.15	1.80	1.80	50.00
	$B_{t\text{-}tn}3$	9.00	9.40	3.15	3.20	50.00

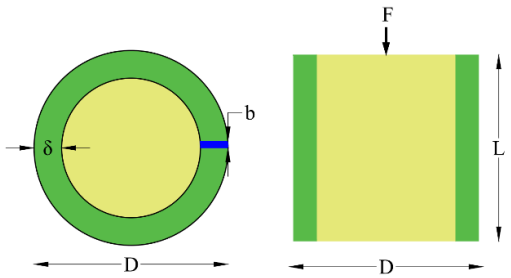

Fig. 3. Compressive test specimen dimension according to ISO 22157:2019.

cross-section detailed in Fig. 7.

3. RESULTS and DISCUSSION

3.1. Tensile test result

Figs. 8–10 present the tensile stress–strain curves of specimens derived from Bamboos 1, 2, and 3, respectively. The curves indicate that the tensile stress parallel to the grain of bamboo exhibits a linear behavior before failure. The ultimate tensile stress values are summarized in Table 3, ranging from 70.13 and 198.42 MPa.

Table 7. Measurement of compressive test specimens

Speciment	Code	Outer diameter (mm)	Inner diameter (mm)	Length (mm)
Bamboo 1	$B_{c\text{-}bi}1$	84.45	60.70	83.90
	$B_{c\text{-}tn}1$	82.13	64.90	80.70
Bamboo 2	$B_{c\text{-}ti}2$	77.58	61.53	79.30
Bamboo 3	$B_{c\text{-}bi}3$	85.05	63.13	85.70
	$B_{c\text{-}tn}3$	72.53	58.20	65.35

Table 8. Outer diameter and the thickness of the bending specimen

Tests specimen	Outer diameter (mm)				Thickness (mm)		
	Bottom	Middle	Top	Average	Bottom	Top	Average
B_{b1}	86.3	84.8	86.2	85.8	14.3	10.1	12.2
B_{b2}	88.4	83.7	83.6	85.2	14.0	9.3	11.7
B_{b3}	82.9	77.8	74.4	78.4	12.3	8.7	10.5

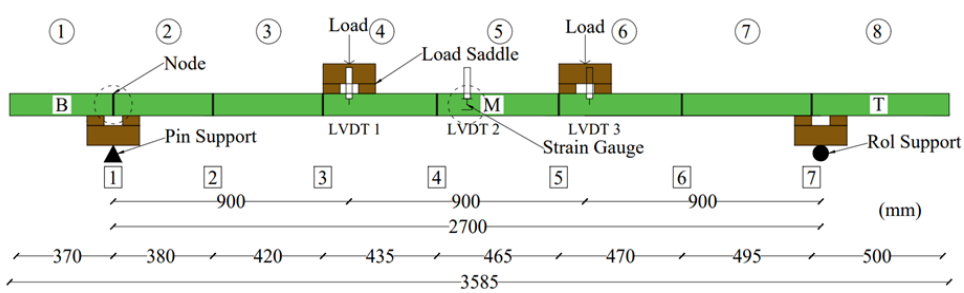

Fig. 4. Bending test setup of B_b1.

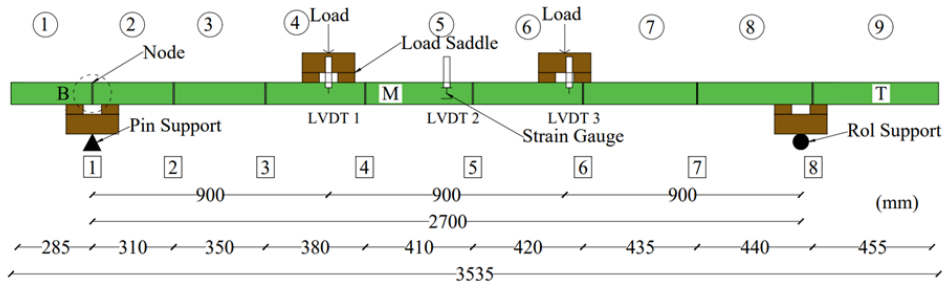

Fig. 5. Bending test setup of B_b2.

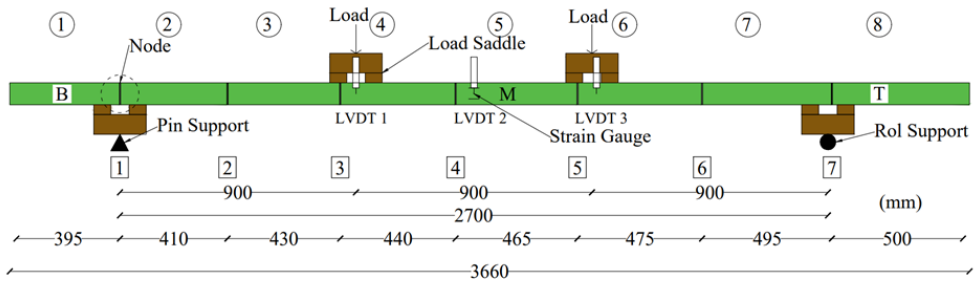

Fig. 6. Bending test setup of B_b3.

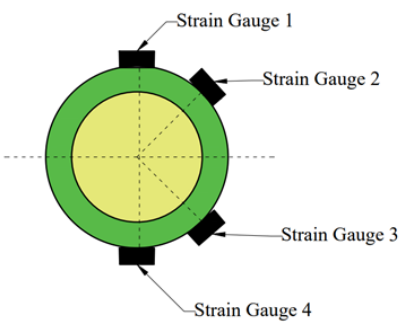

Fig. 7. Strain gauge position at the cross-section.

For Bamboo 1, the average ultimate tensile stresses of the internode and node regions were 118.08 MPa and 75.76 MPa, respectively. For Bamboo 3, the corresponding values were 177.88 MPa and 77.43 MPa. Due to specimen limitations, averaging could not be conducted for Bamboo 2; however, the ultimate tensile stresses for its internode and node parts were 198.35 MPa and 125.12 MPa, respectively. Across all specimens, the average ultimate tensile stresses of the internode and node parts were 164.77 MPa and 92.77 MPa, respectively, indicating that the internode part consistently demonstrated higher tensile strength than the node part.

The tensile elastic modulus of Wulung bamboo is presented in Table 9, awith values ranging from 9,631 to 18,400 MPa. The average modulus was determined by combining two stress–strain data pairs obtained from the bottom and part of the bamboo culm of each internode or node section of the bamboo culm. Linear regression was then applied to these combined data to calculate the average tensile elastic modulus. For Bamboo 1, the average tensile elastic modulus parallel to the grain was 16,436 MPa for the internode region and 10,607 MPa for the node region. For Bamboo 3, the corresponding values were 14,804 MPa and 12,141 MPa. Due to data limitations, averaging could not be performed for Bamboo 2; however, its tensile elastic moduli for the internode and node regions were 16,126

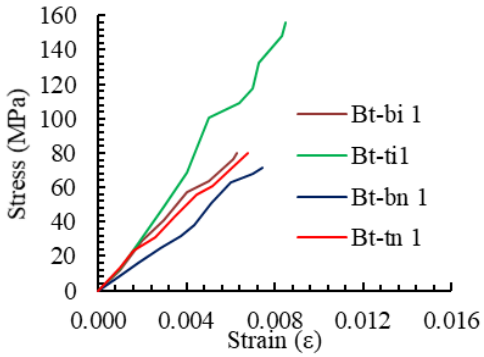

Fig. 8. Tensile stress–strain curve of Bamboo 1.

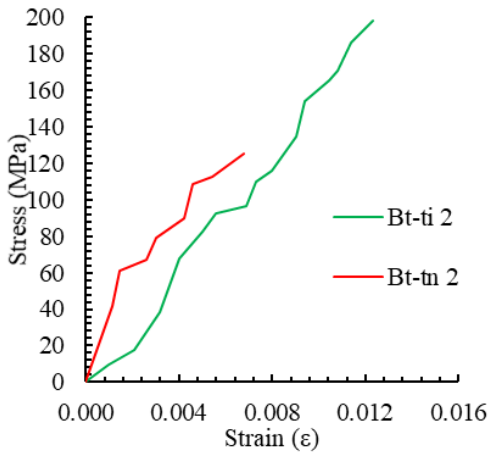

Fig. 9. Tensile stress–strain curve of Bamboo 2.

MPa and 18,400 MPa, respectively. Across all specimens, the average tensile elastic modulus parallel to the grain was 15,789 MPa for the internode and 13,716 MPa for the node, indicating that the internode consistently exhibited a higher modulus than the node.

The variability of the tensile test results is presented in Table 10 and was evaluated using the coefficient of variation (CoV). In contrast to the previous calculation of average tensile strength and elastic modulus, where values were determined individually for each bamboo specimen (Bamboo 1, Bamboo 2, and Bamboo 3), the variability analysis in this section was performed by

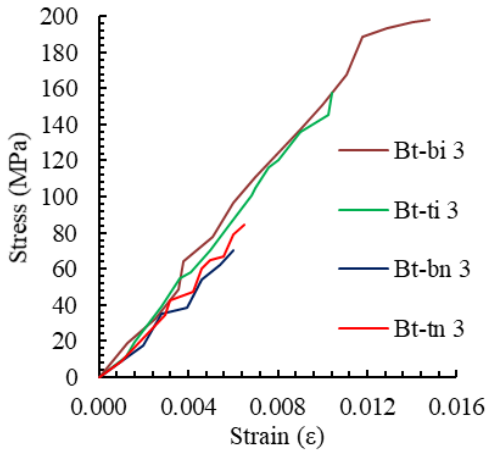

Fig. 10. Tensile stress–strain curve of Bamboo 3.

grouping the data into two categories: specimens with and specimens without nodes. Consequently, each group consisted of five samples.

Table 10 shows that the CoV for tensile strength at the internode and node parts were 30.58% and 26.08%, respectively. The CoV for tensile modulus of elasticity at internode and node were 13.21% and 25.41%, respectively. Comparison with previous studies, also presented in Table 10, indicates that larger sample sizes do not necessarily result in lower variability in tensile properties. Two primary factors may account for this observation. First, the small cross-sectional dimensions of the tensile specimens may contribute to higher variability. Second, the irregular distribution of fibers, as noted by Al-Rukaibawi and Károlyi (2023), can also influence the results. Fiber density in bamboo varies not only along the longitudinal axis but also radially. As a result, small specimens may fail to capture representative fiber density across the bamboo cross-section, leading to greater dispersion in the measured tensile properties.

3.2. Compresive test result

Figs. 11–13 present the compressive stress–strain

Table 9. Ultimate tensile stress and elastic tensile modulus

Specimen	$\sigma_{ultimate}$ (MPa)			Tensile modulus of elasticity E_T (MPa)		
	Bamboo 1	Bamboo 2	Bamboo 3	Bamboo 1	Bamboo 2	Bamboo 3
$B_{t\text{-}bi}$	80.03	-	198.42	12,937	-	13,407
$B_{t\text{-}ti}$	156.13	198.35	157.34	17,799	16,126	15,129
$B_{t\text{-}bn}$	71.71	-	70.13	9,631	-	11,688
$B_{t\text{-}tn}$	79.81	125.12	84.73	11,974	18,400	13,036

Table 10. Comparison of data variation

	Research result conducted by	This research	Hoque *et al.* (2019)	Cui *et al.* (2024)	Meng *et al.* (2023)	Liu *et al.* (2021)
Tensile σ ultimate (MPa)	Number of sample without node	5	3	320	6	147
	CoV internode	30.58%	10.38%	24.50%	5.42%	6.30%
	Number of sample with node	5	3	-	6	167
	CoV node	26.08%	9.05%	-	9.36%	8.80%
Tensile modulus of elasticity ET (MPa)	Number of sample without node	5	3	320	-	-
	CoV internode	13.21%	4.12%	15.40%	-	-
	Number of sample with node	5	3	-	-	-
	CoV node	25.41%	14.08%	-	-	-
Compressive σ ultimate (MPa)	Number of sample without node	3	4	-	12	231
	CoV internode	6.76%	9.47%	-	7.05%	8.20%
	Number of sample with node	2	4	-	12	74
	CoV node	0.81%	25.76%	-	9.16%	6.90%
Compressive modulus of elasticity EC (MPa)	Number of sample without node	3	4	-	-	231
	CoV internode	20.25%	40.03%	-	-	8.70%
	Number of sample with node	2	4	-	-	74
	CoV node	11.25%	52.67%	-	-	8.00%

CoV: coefficient of variation.

curves of specimens derived from Bamboos 1, Bamboo 2, and Bamboo 3, respectively. These curves indicate that Wulung bamboo exhibits plastic behavior under compressive loading. The compressive elastic limit and ultimate stress values for each bamboo specimen are summarized summarized in Table 11.

The average compressive elastic limit stresses of the internode and node parts were 43.32 MPa and 42.90 MPa, respectively. The corresponding average ultimate compressive stresses were 53.71 MPa and 51.30 MPa. These results indicate that the internode part tends to exhibit slightly higher compressive strength than the

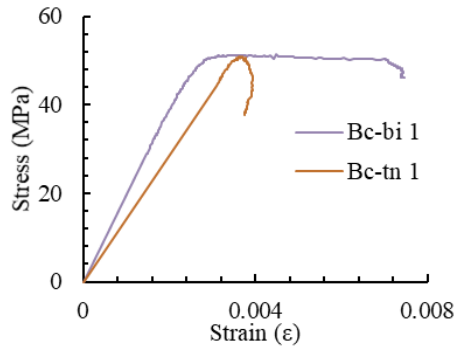

Fig. 11. Compressive stress–strain curve of the specimen made of Bamboo 1.

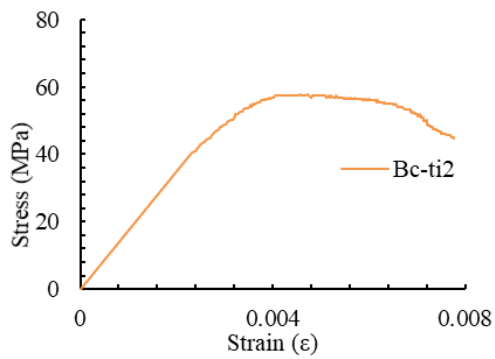

Fig. 12. Compressive stress–strain curve of the specimen made of Bamboo 2.

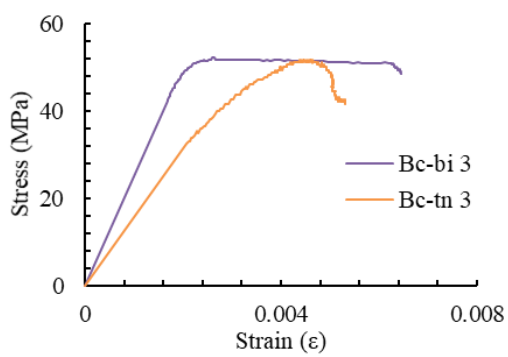

Fig. 13. Compressive stress–strain curve of the specimen made of Bamboo 3.

node part.

Figs. 11–13 also illustrate that the compressive ductility of the internode part of bamboo is greater than that of the node part of bamboo. This observation is supported by the corresponding ductility index values, which are presented in Table 11. The average ductility indices of the internode and node parts were 1.894 and 1.108, respectively, confirming that the internode section of the bamboo exhibits higher compressive ductility.

The compressive elastic modulus parallel to the grain was determined from the compressive stress–strain curves, as presented in Table 11. The procedure for calculating the compressive elastic modulus differs slightly from that used for the tensile modulus. Unlike in the tensile test, the data from the top and bottom parts of each bamboo specimen were not combined due to data limitations in the compression test. For Bamboo 1, the compressive elastic moduli of the internode and node part were 19,800 MPa and 14,050 MPa, respectively. For Bamboo 2, only the internode modulus was obtained, with a value of 17,889 MPa. For Bamboo 3, the internode and node moduli were 26,120 MPa and 16,478 MPa, respectively. The average compressive elastic modulus parallel to the grain for the internode and node parts across all specimens was 21,270 MPa and 15,264 MPa, respectively. These results indicate that the internode part consistently exhibits higher compressive stiffness than the node part.

The variability of the compressive modulus and compressive strength is summarized in Table 10, where the data are categorized into two groups: internode specimens and node specimens. The compression tests were conducted on three internode samples and two node samples. The results show that the CoV for compressive strength was 6.76% for internodes and 0.81% for nodes. Meanwhile, the CoV for the compressive modulus of elasticity were 20.25% and 8.70% for internodes and nodes, respectively.

The number of compression test specimens was comparable to that of the tensile test specimens. However, the compressive mechanical properties exhibited greater

Table 11. Compressive elastic limit, ultimate stress, ductility index, and elastic compressive modulus

Bamboo	Specimen	$\sigma_{elastic\text{-}limit}$ (MPa)	$\sigma_{ultimate}$ (MPa)	Ductility index	Compressive modulus of elasticity E_C (MPa)
Bamboo 1	$B_{c\text{-}bi}1$	45.71	51.19	1.660	19,800
	$B_{c\text{-}tn}1$	49.34	51	1.052	14,050
Bamboo 2	$B_{c\text{-}ti}2$	41.87	57.87	1.582	17,889
Bamboo 3	$B_{c\text{-}bi}3$	42.37	52.07	2.439	26,120
	$B_{c\text{-}tn}3$	36.45	51.59	1.164	16,478

homogeneity than the tensile properties. This can be attributed to the fact that compressive loading engages a larger portion of the bamboo structure, whereas tensile loading primarily acts on a limited number of fibers within the cross-section. The larger dimensions of the compression specimens allow for a more representative assessment of the material's average compressive behavior, thereby minimizing the influence of local variations and resulting in reduced data dispersion compared to the tensile test results.

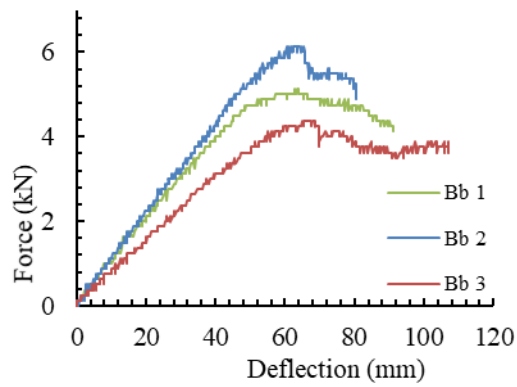

Fig. 14. Load–displacement curve of bending test.

3.3. Bending test result

3.3.1. Load-deflection curve and failure mode

The load–deflection curves of B_b1, B_b2, and B_b3 are presented in Fig. 14. Each curve shows that the deflection of the bamboo increased linearly with load up to the elastic limit. As the load continued to increase, the deflection exhibited nonlinear growth until the ultimate load was reached. Beyond this point, the load gradually decreased.

The elastic limit load, elastic limit deflection, ultimate load, and bending elastic modulus of the three bamboo specimens are summarized in Table 12. The bending elastic modulus was determined from the slope of the load–deflection curve within the elastic range. As shown in Table 12, the average bending elastic modulus of bamboo was 18,120 MPa, with a CoV of 2.87%.

Figs. 15–17 illustrate the observed failure modes of Bamboos 1, 2, and 3, respectively. The bending failures of B_b1 (Fig. 15) and B_b3 (Fig. 17) occurred beneath the right saddle, near the top side of the specimen. In contrast, the failure of B_b2 (Fig. 16) occurred beneath the left saddle, also near the top. All specimens exhibited local buckling followed by longitudinal splitting along both edges of the bamboo culm.

Local buckling occurred because the saddle was not positioned directly over a bamboo node. Theoretically, aligning the saddle with a node can help prevent buckling. However, due to the natural variability in node spacing along the bamboo culm, consistently aligning the saddle with a node is challenging in practice. The buckling test was conducted in accordance with ISO 22157:2019, as illustrated in Fig. 18, which shows that the saddle was not precisely aligned with a node. The

Table 12. Bending test result data of B_b1, B_b2, and B_b3

Specimen	$P_{elastic\text{-}limit}$ (kN)	$\Delta_{elastic\text{-}limit}$ (mm)	$P_{ultimate}$ (kN)	MoE_b (MPa)	MoR (MPa)
B_b1	4.75	8.475	5.125	17,563	50.460
B_b2	5.875	6.25	6.125	18,594	62.867
B_b3	3.5	5.45	4.375	18,203	58.452
Average MoE_b (MPa)				18,120	57
Standard deviation (MPa)				520	6
Variation of coefficient				2.87%	10.98%

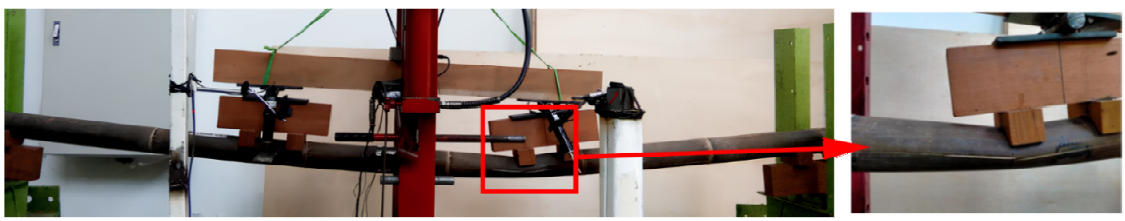

Fig. 15. Failure mode of Bamboo 1.

Fig. 16. Failure mode of Bamboo 2.

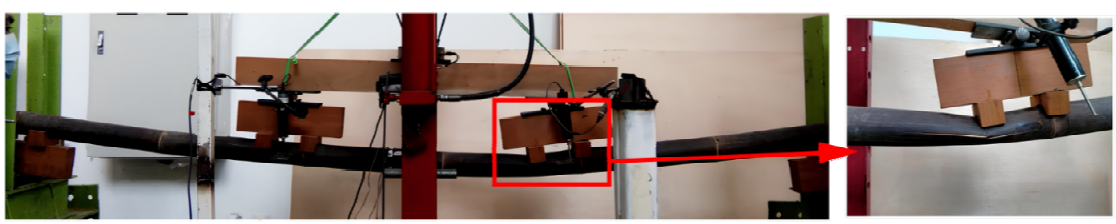

Fig. 17. Failure mode of Bamboo 3.

occurrence of local buckling influenced the bending behavior of the bamboo beam by reducing its lateral load-carrying capacity. Nonetheless, this buckling had minimal effect on the strain measurements in this study, as it occurred near the saddle—approximately one-third of the span—whereas the strain gauges were installed at

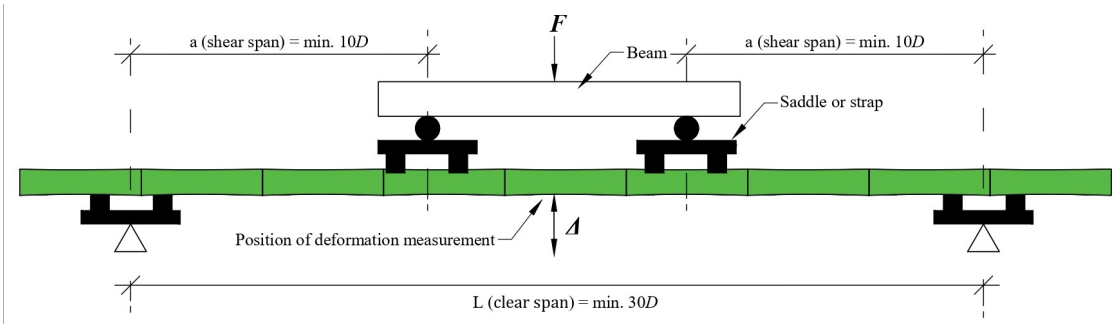

Fig. 18. Schematic of bending test according to ISO 22157:2019.

mid-span, away from the buckling zone.

3.3.2. Strain distribution and neutral axis position

The strain distribution curves of specimens B_b1, B_b2, and B_b3 under lateral loading from 1 kN to the ultimate load are presented in Figs. 19–21, respectively. In all cases, the strain distribution remained approximately linear, even beyond the elastic limit. These curves were used to determine the position of the neutral axis at various load levels. The neutral axis was identified as the location along the cross-section where the longitudinal strain equaled zero, and its position was measured relative to the mid-diameter of the bamboo culm. As shown in Figs. 19–21, the neutral axis positions of Bamboos 1, 2, and 3 at different loading stages are summarized in Table 13. Notably, the neutral axis position varied with increasing load and tended to shift away from the centroid of the cross-section. Overall, the

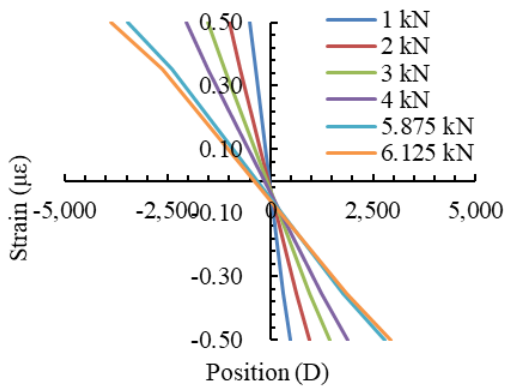

Fig. 20. Strain distribution of B_b2.

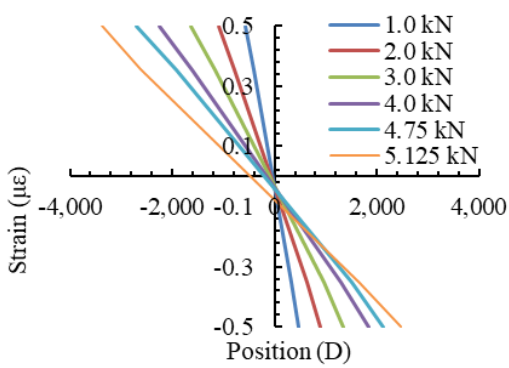

Fig. 19. Strain distribution of B_b1.

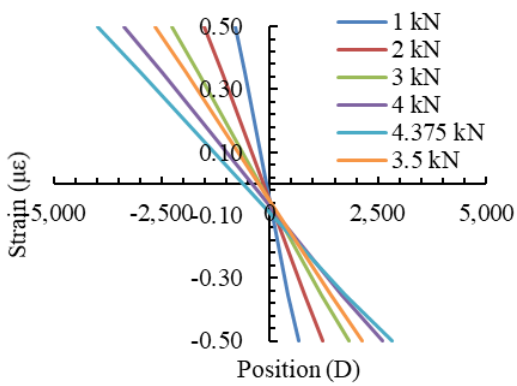

Fig. 21. Strain distribution of B_b3.

Table 13. Neutral axis position of bamboo

Bamboo 1			Bamboo 2			Bamboo 3		
Load (kN)	Neutral axis		Load (kN)	Neutral axis		Load (kN)	Neutral axis	
	(D)*	(mm)		(D)*	(mm)		(D)*	(mm)
1	−0.03	−2.57	1	−0.03	−2.19	1	−0.05	−4.3
2	−0.04	−2.98	2	−0.03	−2.43	2	−0.06	−4.37
3	−0.03	−2.75	3	−0.03	−2.52	3	−0.06	−4.37
4	−0.04	−3.25	4	−0.03	−2.92	3.5**	−0.06	−4.39
4.750**	−0.04	−3.43	5.875**	−0.05	−4.47	4	−0.07	−5.4
5.125***	−0.08	−6.61	6.125***	−0.06	−5.17	4.375***	−0.09	−7.17

* D is bamboo diameter, ** Elastic limit load, *** Ultimate load.

compressive strain zone was consistently larger than the tensile strain zone, indicating an asymmetric flexural response of the bamboo culm.

The neutral axis does not lie at the mid-diameter of the bamboo cross-section due to the difference between the tensile and compressive moduli of elasticity parallel to the grain. For the internode region, the average tensile and compressive moduli are 15,789 MPa and 21,270 MPa, respectively. In the node region, the corresponding values are 13,716 MPa and 15,264 MPa.

The reduced stiffness in the node area is attributed to both microstructural and morphological factors. The discontinuity and interruption of longitudinal fibers within the node restrict the efficiency of stress transfer, particularly under tensile loading (Chen and Luo, 2020). Moreover, the irregular and multidirectional fiber orientations in the node region leads to localized stress concentrations and deformation, thereby diminishing its structural integrity (Meng *et al.*, 2023).

Further analysis of the neutral axis position focused on the tensile and compressive properties parallel to the grain in the internode part, as the strain gauges were installed in this section of the bamboo culm. The results indicate that the tensile elastic modulus in the internode is lower than its compressive counterpart, consistent with findings reported by Gauss *et al.* (2019). However, the observed position of the neutral axis—located below the mid-height of the cross-section—would theoretically suggest that the tensile modulus should exceed the compressive modulus.

The discrepancy between the tensile-to-compressive modulus ratio and the observed neutral axis position can be attributed to two primary factors. First, bamboo is an inherently non-homogeneous material, with mechanical properties that vary along its length due to differences in fiber distribution, density, and anatomical structure between nodes and internodes. Second, tensile, compressive, and bending specimens could not be extracted from the same longitudinal location along the culm due to dimensional constraints. This limitation poses a significant challenge in structural bamboo research, particularly when attempting to establish a direct correlation between the neutral axis position and the tensile and compressive moduli of elasticity parallel to the grain.

In addition, this study conducted an analysis of strain distribution, stress distribution, and the equilibrium of normal forces at the cross-section where the strain gauges were installed. The stress distributions for specimens B_b1, B_b2, and B_b3 under various loading condi-

tions are presented in Figs. 22–24. These distributions were derived from the average stress–strain relationships obtained from the tensile and compressive tests parallel to the grain in the internode region of each bamboo culm and correlated with the strain distributions across the respective cross-sections (Figs. 19–21). Within the

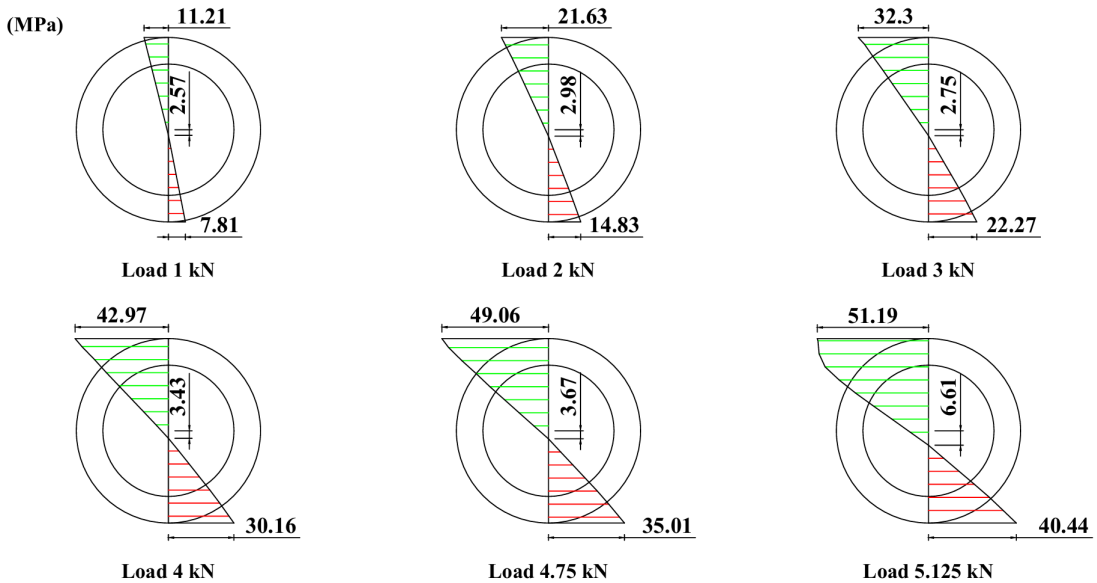

Fig. 22. The cross-section stress distribution at the middle span of Bamboo 1.

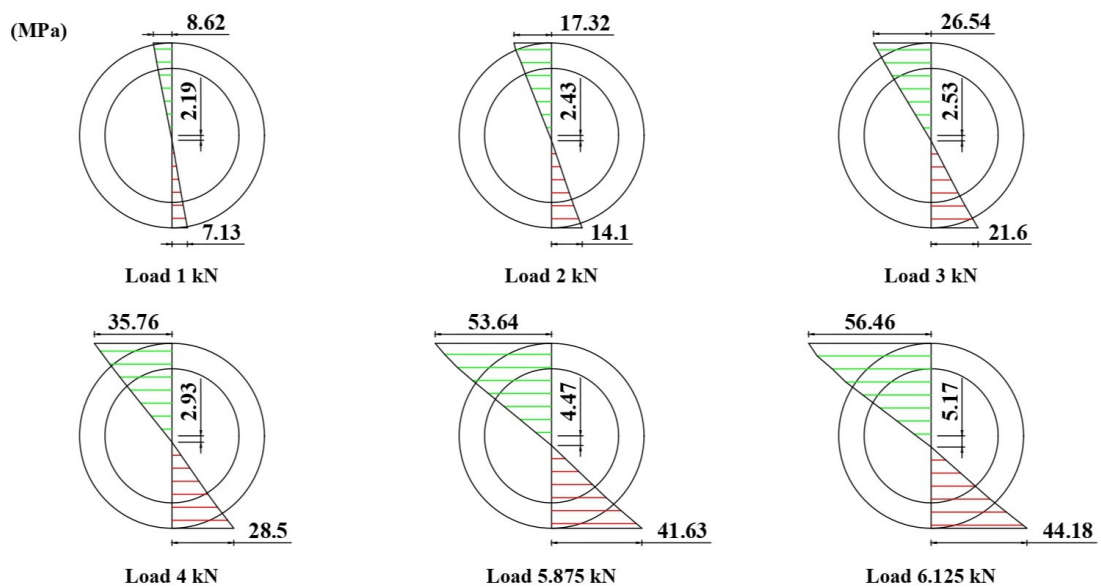

Fig. 23. The cross-section stress distribution at the middle span of Bamboo 2.

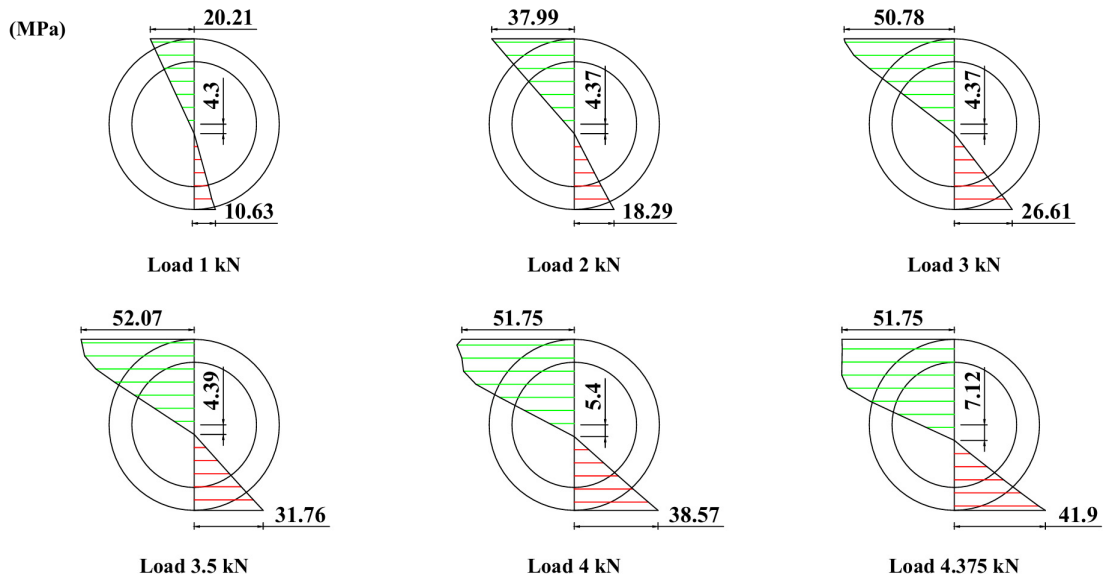

Fig. 24. The cross-section stress distribution at the middle span of Bamboo 3.

linear range, the stress–strain relationship was defined by the average modulus of elasticity, as shown in Table 14. Based on these stress distributions, the axial tensile force the axial tensile F_T and compressive forces F_C were calculated. The results are presented in Tables 15–17 for Bamboos 1, 2, and 3, respectively.

The results indicate that the resultant axial force (ΣF) does not equal zero when the axial tensile F_T and compressive F_C forces are calculated using the original tensile and compressive moduli of elasticity obtained from the tests. Theoretically, the resultant axial force must be zero. As previously discussed, when the neutral axis shifts downward, the tensile modulus should exceed the compressive modulus to achieve axial force equilibrium. To address this discrepancy, a modification factor was introduced in this study. The applied modification factors and the corresponding adjusted axial force results are presented in Tables 15–17. By applying this factor, the tensile modulus becomes greater than the compressive modulus, thereby bringing the resultant axial force closer to zero. Further detailed analysis using finite element modeling is recommended to simulate the interaction between neutral axis position, the modified tensile and compressive moduli of elasticity parallel to

Table 14. Average modulus of elasticity

Bamboo	E_T internode (MPa)	Average E_T internode (MPa)	E_C internode (MPa)
B_{b1}	12,937 17,799	15,368	19,800
B_{b2}	16,126	16,126	17,889
B_{b3}	13,407 15,129	14,268	26,120

Table 15. Equilibrium normal force before and after using purpose modification factor of Bamboo 1

Load (kN)	Original F_T (kN)	Original F_C (kN)	Original ΣF (kN)	Modification factor		Modified F_T (kN)	Modified F_C (kN)	Modified ΣF (kN)
	(1)	(2)	(1) + (2)	Compression	Tension	(3)	(4)	(3) + (4)
1	−8.99	5.67	−3.32	0.79	1.24	−7.11	7.09	−0.02
2	−17.11	10.89	−6.22			−13.52	13.61	0.10
3	−25.44	16.53	−8.91			−20.10	20.66	0.56
4	−35.21	22.10	−13.11			−27.81	27.62	−0.19

Table 16. Equilibrium normal force before and after using purpose modification factor of Bamboo 2

Load (kN)	Original F_T (kN)	Original F_C (kN)	Original ΣF (kN)	Modification factor		Modified F_T (kN)	Modified F_C (kN)	Modified ΣF (kN)
	(1)	(2)	(1) + (2)	Compression	Tension	(3)	(4)	(3) + (4)
1	−6.86	2.50	−4.35	0.59	1.65	−4.01	4.00	−0.01
2	−13.83	4.92	−8.91			−8.09	7.87	−0.22
3	−21.13	7.50	−13.63			−12.36	12.00	−0.36
4	−28.62	9.81	−18.82			−16.74	15.69	−1.05

Table 17. Equilibrium normal force before and after using purpose modification factor of Bamboo 3

Load (kN)	Original F_T (kN)	Original F_C (kN)	Original ΣF (kN)	Modification factor		Modified F_T (kN)	Modified F_C (kN)	Modified ΣF (kN)
	(1)	(2)	(1) + (2)	Compression	Tension	(3)	(4)	(3) + (4)
1	−13.71	2.72	−10.99	0.50	2.49	−6.86	6.79	−0.07
2	−25.79	5.14	−20.65			−12.89	12.85	−0.04
3	−37.70	7.63	−30.07			−18.85	19.08	0.23

the grain, and the overall bending behavior of bamboo.

3.4. Review of structural bamboo design based on ISO 22156:2021

In the structural design of bamboo beams based on ISO 22156:2021, the allowable lateral load is primarily determined by the flexural strength, while axial tensile and compressive strengths are generally not considered. However, ISO 22156:2021 does not yet specify the correction factors, as specified in the timber structural standard code. Thus, a review of bamboo beam design in this study was conducted by calculating the allowable lateral load for each specimen using the Load and Resistance Factor Design (LRFD) method. The flexural strength values of Bamboos 1, 2, and 3 were used as their respective reference strengths. A flexural resistance factor (ϕ) of 0.85 was applied, in accordance with SNI 7973:2013, which is adapted from NDS 2012. All modification factors—including wet service, temperature,

beam stability, size, flat use, incising, repetitive member, format conversion, and time effect factor—were assumed to be equal to 1.0. The allowable lateral loads were then calculated following ISO 22156:2021 and are summarized in Table 18. As shown, the calculated values remain below the corresponding experimental elastic limit loads. This indicates that the normal stress distribution parallel to the fibers remains linear and that the structural response of the bamboo beams remains within the elastic range. Considering these calculation results, ISO 22156:2021 can be appropriately applied at the design stage, provided that the material behavior remains within the linear elastic domain. Nevertheless, incorporating a more detailed analysis of the actual stress-strain distribution along the fiber direction would help support and refine the structural design process.

4. CONCLUSIONS

The average tensile modulus of elasticity parallel to the fibers of Wulung bamboo was 15,789 MPa for internodes and 13,716 MPa for nodes, whereas the average compressive modulus of elasticity in the same direction was 21,270 MPa and 15,264 MPa, respectively. This disparity between tensile and compressive stiffness leads to a shift in the neutral axis position when the bamboo is subjected to lateral loading, causing it to deviate from the centroid of the cross-section.

The results of the bending tests indicate that the strain distribution across the bamboo cross-section remains linear, even beyond the elastic limit. The neutral axis was consistently observed below the geometric center of the cross-section. Moreover, the position of the neutral axis shifted downward as the magnitude of lateral loading increased. When the applied load remained within the elastic range, the stress distribution was also linear throughout the cross-section. However, once the load exceeded the elastic limit, the stress distribution became nonlinear, particularly in the compressive region above the neutral axis.

The experimental results revealed that the average tensile modulus of elasticity is lower than the average compressive modulus of elasticity. Nevertheless, the neutral axis was found to lie below the centroid of the bamboo cross-section. Theoretically, such a position implies that the tensile modulus should exceed the compressive modulus in order to achieve equilibrium of internal normal forces within the beam. To address this inconsistency, a modification factor for the elastic moduli was introduced in this study to ensure a balanced stress distribution and satisfy equilibrium conditions in flexural analysis.

The observation of bending behavior, particularly in establishing a direct correlation between the neutral axis position and the tensile and compressive moduli of elasticity parallel to the grain, presents significant challenges. One of the main obstacles is the limitation of specimen dimensions, which makes it difficult to obtain tensile and compressive specimens parallel to the grain from the exact location where strain gauges are installed. Furthermore, bamboo is inherently non-homogeneous in both the radial and longitudinal directions,

Table 18. The comparison between allowable lateral load and load obtain from experiment

Specimen	Experiment result			Allowable lateral load (kN)
	$P_{elastic\text{-}limit}$ (kN)	$\Delta_{elastic\text{-}limit}$ (mm)	$P_{ultimate}$ (kN)	
B_b1	4.75	8.475	5.125	4.356
B_b2	6.00	6.250	6.125	5.206
B_b3	3.50	5.450	4.375	3.719

further complicating accurate characterization of its mechanical behavior.

Further finite element analysis is recommended to simulate the interaction between the neutral axis position, the modified tensile and compressive moduli of elasticity parallel to the grain, and the overall bending behavior of bamboo. This simulation should incorporate the proposed modification factors introduced in this study. These modification factors can be applied to the constitutive equation of bamboo as input material properties to more accurately represent its mechanical response under flexural loading.

Based on the design review conducted in accordance with ISO 22156:2021, the calculated allowable loads remain within the linear range, and the structural response of the bamboo beams remains in the elastic domain. These results suggest that ISO 22156:2021 can be reliably applied during the design phase, provided that the material behavior does not exceed the linear elastic range. However, incorporating a more detailed analysis of the actual stress–strain distribution along the fiber direction would further enhance the accuracy and reliability of the structural design process.

CONFLICT of INTEREST

No potential conflict of interest relevant to this article was reported.

ACKNOWLEDGMENT

We acknowledge the Department of Civil and Environmental Engineering Universitas Gadjah Mada for assisting with the equipment during the experimental test.

REFERENCES

Al-Rukaibawi, L.S., Károlyi, G. 2023. Through-thickness distribution of bamboo tensile strength parallel to fibres. SN Applied Sciences 5(7): 174.

Awaludin, A., Shulhan, M.A., Effendi, M.K., Irawati, I.S., Hassan, R. 2025. Flexural properties of structural size glulam beams made from Indonesian wood species: Experimental programs. Journal of the Korean Wood Science and Technology 53(3): 287-300.

Cai, X., Wang, M., Lu, Y., Noori, A., Chen, J., Chen, F., Chen, L., Jiang, X., Zhang, Q. 2023. Experimental study on the dynamic tensile failure of bamboo. Construction and Building Materials 392: 131886.

Chen, G., Luo, H. 2020. Effects of node with discontinuous hierarchical fibers on the tensile fracture behaviors of natural bamboo. Sustainable Materials and Technologies 26: e00228.

Cui, Z., Jiao, Z., Tong, W. 2024. Design value of tensile strength of raw bamboo. BioResources 19(1): 944-954.

De Jesus, A.P., Garciano, L.E., Lopez, L., Ong, D.M., Chrissel Paula Roxas, M., Tan, M.A., De Jesus, R. 2021. Establishing the strength parameters parallel to fiber of *Dendrocalamus Asper* (giant bamboo). International Journal of GEOMATE 20(81): 22-27.

Deng, Y., Peng, C. 2021. Experimental study on bending mechanical properties of moso bamboo. E3S Web of Conferences 293: 03010.

Eratodi, I.G.L.B. 2017. Buku Struktur dan Rekayasa Bambu. Universitas Pendidikan Nasional, Denpasar, Indonesia.

Fitrianto, A. 2015. Bamboo architecture for sustainable communities. International Conference: Parahyangan Bamboo Nation 2: 1-8.

Galih, N.M., Yang, S.M., Yu, S.M., Kang, S.G. 2020. Study on the mechanical properties of tropical hybrid cross laminated timber using bamboo laminated board as core layer. Journal of the Korean Wood Science and Technology 48(2): 245-252.

Gauss, C., Savastano, H. Jr., Harries, K.A. 2019. Use of

ISO 22157 mechanical test methods and the characterisation of Brazilian *P. edulis* bamboo. Construction and Building Materials 228: 116728.

Gunawan, I., Sugiartha, I.W., Anshari, B. 2015. Pengaruh ekstrak daun mimba sebagai bahan alami pengawet bambu terhadap sifat mekanik bambu petung. Spektrum Sipil 2(1): 1-11.

Hartono, R., Iswanto, A.H., Priadi, T., Herawati, E., Farizky, F., Sutiawan, J., Sumardi, I. 2022. Physical, chemical, and mechanical properties of six bamboo from Sumatera Island Indonesia and its potential applications for composite materials. Polymers 14(22): 4868.

Hoque, M., Islam, M.N., Manjur, K.A., Anis, M. 2019. Experimental investigation on the mechanical properties of bamboo in Bangladesh. DUET Journal 5(1): 37-43.

International Organization for Standardization. 2019. Bamboo Structures: Determination of Physical and Mechanical Properties of Bamboo Culms: Test Methods. ISO 22157. International Organization for Standardization, Geneva, Switzerland.

International Organization for Standardization. 2021a. Bamboo Structures: Bamboo Culms: Structural Design. ISO 22156. International Organization for Standardization, Geneva, Switzerland.

International Organization for Standardization. 2021b. Timber Structures. ISO/TC 165. International Organization for Standardization, Geneva, Switzerland.

Irnawan, D. 2022. Bambu sebagai material konstruksi yang mudah dibentuk pada konstruksi bangunan menara penangkap embun. Jurnal Teknosains Kodepena 2(2): 27-31.

Iswanto, A.H., Hakim, A.R., Azhar, I., Wirjosentono, B., Prabuningrum, D.S. 2020. The physical, mechanical, and sound absorption properties of sandwich particleboard (SPb). Journal of the Korean Wood Science and Technology 48(1): 32-40.

Kim, C.K., Kim, K.M., Lee, S.J., Park, M.J. 2018. Change of bending properties of 2×4 larch Lumber according to span length in the four point bending test. Journal of the Korean Wood Science and Technology 46(5): 486-496.

Lapina, A.P., Zakieva, N.I. 2021. Bamboo in modern construction and architecture. IOP Conference Series: Materials Science and Engineering 1083(1): 012019.

Lee, I.H., Pack, J., Song, D., Hong, S. 2018. Longitudinal bonding strength performance evaluation of larch lumber. Journal of the Korean Wood Science and Technology 46(1): 85-92.

Li, J., Singh, A., Zhou, Y. 2024. Experimental study on the flexural behavior of I-shaped laminated bamboo composite beam as sustainable structural element. Buildings 14(3): 671.

Liu, P., Zhou, Q., Fu, F., Li, W. 2021. Effect of bamboo nodes on the mechanical properties of *P. edulis* (*Phyllostachys edulis*) bamboo. Forests 12(10): 1309.

Lubis, R.O.O.P. 2019. Sifat Mekanika dan Fisika Bambu Wulung (Studi Kasus: Bambu Daerah Seyegan). Universitas Gadjah Mada, Yogyakarta, Indonesia.

Maulana, S., Gumelar, Y., Fatrawana, A., Maulana, M.I., Hidayat, W., Sumardi, I., Wistara, N.J., Lee, S.H., Kim, N.H., Febrianto, F. 2019. Destructive and non-destructive tests of bamboo oriented strand board under various shelling ratios and resin contents. Journal of the Korean Wood Science and Technology 47(4): 519-532.

Medina Yor Maikol, S., Vasily Maksimovich, S., Galina Ivanovna, B., Ainur, S. 2020. Bamboo structures for modern sustainable architecture. ISVS E-Journal 7(3): 27-39.

Meng, X., Zhang, Z., Wu, Y., Xu, F., Feng, P. 2023. A comprehensive evaluation of the effects of bamboo nodes on the mechanical properties of bamboo culms. Engineering Structures 297: 116975.

Ready, B., Krisnamurti, Nurtjahjaningtyas, I. 2020. Analysis of slope stability in soft soil using hardening soil modeling and strengthening of bamboo

mattress. International Journal of GEOMATE 19(73): 226-234.

Rofii, M.N., Mairing, M.J., Listyanto, T., Sumardi, I., Hartono, R. 2024. Physical and mechanical properties of laminated board from betung bamboo (*Dendrocalamus asper*). Journal of the Korean Wood Science and Technology 52(4): 383-392.

Sumardi, I., Alamsyah, E.M., Suhaya, Y., Dungani, R., Sulastiningsih, I.M., Pramestie, S.R. 2022. Development of bamboo zephyr composite and the physical and mechanical properties. Journal of the Korean Wood Science and Technology 50(2): 134-147.

Tian, L., Wei, J., Hao, J., Wang, Q. 2021. Characterization of the flexural behavior of bamboo beams. Journal of Renewable Materials 9(9): 1571-1597.

Wang, F., Ding, S., Wu, Y., Zhang, C., Zhang, T., Shao, Z., Guo, Y., Chen, Y., Xie, H., Zhang, E. 2023. Study on the influence of node part on the bending behaviors of bamboo. Industrial Crops and Products 204: 117384.

Widoyoko, T.A. 2018. Pengaruh Posisi Batang pada Sifat Fisika dan Mekanika Bambu (Studi Kasus Bambu Wulung dari Wilayah Margoagung). Universitas Gadjah Mada, Yogyakarta, Indonesia.

Zhang, X., Zhao, M., Zhao, E., Li, S., Liu, Q., Yue, Q. 2024. Experimental investigation on duration of load effect of novel inorganic-bonded bamboo composite under flexural load. Construction and Building Materials 421: 135688.